Article:
Zamboni, E, Lowndes, R, Bertamini, M et al. (2026) fMRI responses to horizontal and vertical symmetry axes in ascending visual hierarchy. Neuroimage. 121847. ISSN: 1053-8119

https://doi.org/10.1016/j.neuroimage.2026.121847

NeuroImage 330 (2026) 121847

Contents lists available at ScienceDirect

NeuroImage

journal homepage: www.elsevier.com/locate/ynimg

fMRI responses to horizontal and vertical symmetry axes in ascending visual hierarchy

E. Zamboni [a,b,*], R. Lowndes [b,c,d], M. Bertamini [e,f], A.D.J. Makin [f], A.B. Morland [b,d,g]

[a] School of Psychology, University of Nottingham, Nottingham, UK
[b] York Neuroimaging Centre, University of York, York, UK
[c] Faculty of Psychology and Educational Sciences, University of Coimbra, Portugal
[d] Department of Psychology, University of York, York, UK
[e] Dipartimento di Psicologia Generale, Università di Padova, Padova, Italy
[f] Department of Psychological Sciences, University of Liverpool, Liverpool, UK
[g] York Biomedical Research Institute, University of York, York, UK

ARTICLE INFO

Keywords:
fMRI
Visual cortex
Visual symmetry
Attention
Orientation
Multi-Voxel pattern analysis

ABSTRACT

Visual regularities such as reflection and translation are known to engage extrastriate visual cortex, but how regularity type, axis orientation, and task demand jointly shape these responses remains unclear. We used functional Magnetic Resonance Imaging (fMRI) to measure univariate and multivariate responses to reflection and translation patterns with vertical or horizontal axis of orientation while participants ($n = 24$, 6 male) performed either a regularity discrimination task or an orientation discrimination task.

Univariate analysis showed that stimulus-evoked responses increased from V3 onwards, with minimal responses in V1-V2. Contrary to classical salience accounts, early dorsal regions (V3, V3a, V3b) responded more strongly to translation than reflection. Orientation effects dissociated across regions: V3a and V3b showed stronger responses to horizontal than vertical axes, whereas LO2 showed the opposite preference. Task effects were limited, with no overall enhancement of responses during regularity discrimination.

Multivariate (searchlight MVPA) analysis revealed reliable decoding of regularity in extrastriate regions and decoding of axis orientation in early visual cortex. Orientation information was reduced in extrastriate regions during regularity discrimination relative to orientation discrimination.

These findings show that responses to visual regularities in human visual cortex depend on regularity type, axis orientation, and task demands, with dorsal and ventral regions showing distinct response profiles.

Key Points:

(1) Symmetry-related responses emerge reliably in extrastriate cortex, with univariate responses to reflection and translation differing the most in early dorsal regions (V3, V3a, V3b).
(2) Representation of reflection and translation differ in extrastriate areas, but only modest evidence supports different representation of axis orientation in early visual cortex (V1).
(3) Task (regularity vs orientation discrimination) had limited influence on univariate or multivariate patterns, indicating symmetry representations in visual cortex are largely task-invariant.

1. Introduction

Many animals can detect visual symmetry and use it to guide adaptive behaviour (for reviews see, Bertamini et al., 2018; Makin et al., 2023; Treder, 2010). Symmetry-related fMRI responses are absent in striate cortex (V1) but emerge consistently in extrastriate area V3. Symmetry activations are often strongest in early ventral stream areas such as V4 and LOC (Audurier et al., 2022; Keefe et al., 2018; Kohler et al., 2016; Sasaki et al., 2005; Tyler et al., 2005; Van Meel et al., 2019; Zamboni et al., 2024).

The extrastriate symmetry response can be measured with electroencephalography (EEG). Both symmetrical and asymmetrical stimuli

* Corresponding author at: School of Psychology, University of Nottingham, Nottingham, NG7 2RD, UK.
E-mail addresses: elisa.zamboni1@nottingham.ac.uk (E. Zamboni), rebecca.lowndes@york.ac.uk (R. Lowndes), marco.bertamini@unipd.it (M. Bertamini), alexis.makin@liverpool.ac.uk (A.D.J. Makin), antony.morland@york.ac.uk (A.B. Morland).

https://doi.org/10.1016/j.neuroimage.2026.121847
Received 2 October 2025; Received in revised form 6 March 2026; Accepted 9 March 2026
Available online 10 March 2026

generate Event Related Potentials (ERPs) at posterior electrodes. However, amplitude is lower for symmetrical stimuli from around 200 ms until the end of the epoch. This symmetry-asymmetry difference wave is referred to as the 'Sustained Posterior Negativity' (SPN). The SPN was first reported by Jacobsen & Höfel (2003) and has since been replicated in numerous ERP studies (Makin et al., 2022), including under conditions where symmetrical and asymmetrical stimuli are highly similar and presented for extremely brief durations (Contemori et al., 2026). Any symmetry manipulations which result in a larger SPN are likely to result in a larger extrastriate fMRI response and vice versa (Palumbo et al., 2015). We also know that more salient visual symmetries generated a larger SPN, and that the SPN is present whether participants attend to regularity or not, although the SPN is often larger during regularity discrimination (Makin et al., 2024, 2020). Most relevant to the current study, we know that reflectional symmetry is more salient than translational symmetry, and reflectional symmetry generates a larger SPN than translational symmetry (Makin et al., 2013, 2014).

Most neuroimaging work suggests that the striate cortex (V1) is not activated by symmetry: V1 responses to symmetrical and asymmetrical stimuli are usually indistinguishable. However, van der Zwan et al. (1998) found that the implicit global axis of a symmetrical dot pattern can induce the same tilt aftereffects as a simple luminance defined line. Furthermore, some aftereffects do not transfer completely between eyes, suggesting they might be partially mediated by monocular cells in V1. Therefore, the striate cortex (V1) may play some role in coding symmetry axis orientation, possibly based on feedback from extrastriate cortex.

Most symmetry perception research has presented stimuli in the frontoparallel plane (e.g., with display monitor viewed face on). These symmetrical stimuli project as symmetrical image onto the retina. However, during naturalistic viewing, symmetrical objects are often seen from alternative perspectives which distort symmetry in the retinal image (Sawada and Pizlo, 2008; Szlyk et al., 1995; van der Vloed et al., 2005). There may be some selective stimulus and task conditions in which the brain can *go beyond* the retinal image and achieve a *view invariant* representation of the symmetrical object.

When view invariance is achieved, the neural distinction between frontoparallel and perspective symmetry may be partially *lost* in some parts of the extrastriate symmetry network, as if frontoparallel and perspective symmetry have become the same thing. For instance, when participants attend to regularity, and sufficient 3D depth cues are available, the SPN is the same from frontoparallel and perspective displays. Conversely, when participants attend to colour, and 3D depth cues are impoverished, the SPN is stronger from frontoparallel than perspective displays. In summary, view invariance appears flexible, and only happens sparingly (Karakashevska, Batterley, et al., 2025, 2025; Karakashevska and Makin, 2024; Keefe et al., 2018; Makin et al., 2015; Rampone et al., 2019).

The concept of view invariance can also apply to 2D rotations within the frontoparallel plane, as well as 3D rotations about the axis. It could be that axis orientation is not so readily decodable in the extrastriate cortex when participants attend to regularity as when they attend to orientation.

In the present fMRI study, we presented two types of regularity; reflection and translation, with two orientations; horizontal and vertical (Fig. 1). On different blocks, participants had to discriminate either regularity (reflection or translation) or orientation (horizontal or vertical).

We initially measured univariate responses in atlas defined regions of interest (ROI). This allowed us to replicate and extend previous univariate findings. Given previous univariate research (e.g. Sasaki et al., 2005), we expected reflection and translation to activate the extrastriate symmetry network. We also expected the extrastriate symmetry response to be stronger for reflection than translation, and stronger during the regularity task than the orientation task.

We also measured Multivariate responses throughout the visual cortex. First, given previous MVPA results (e.g. Zamboni et al., 2024), we expected to decode regularity (reflection vs translation) throughout the extrastriate cortex. Second, given previous tilt-aftereffect results (van der Zwan et al., 1998), we expected to decode axis orientation (horizontal vs vertical) in the striate cortex in both tasks. This would happen if top-down signals filled in a horizontal or vertical axis. Third, based on previous fMRI and ERP results (Keefe et al., 2018; Makin et al., 2015), we expected to decode orientation in extrastriate areas during the orientation task, *but not during the regularity task*. In other words, the distinction between horizontal and vertical regularities should be lost

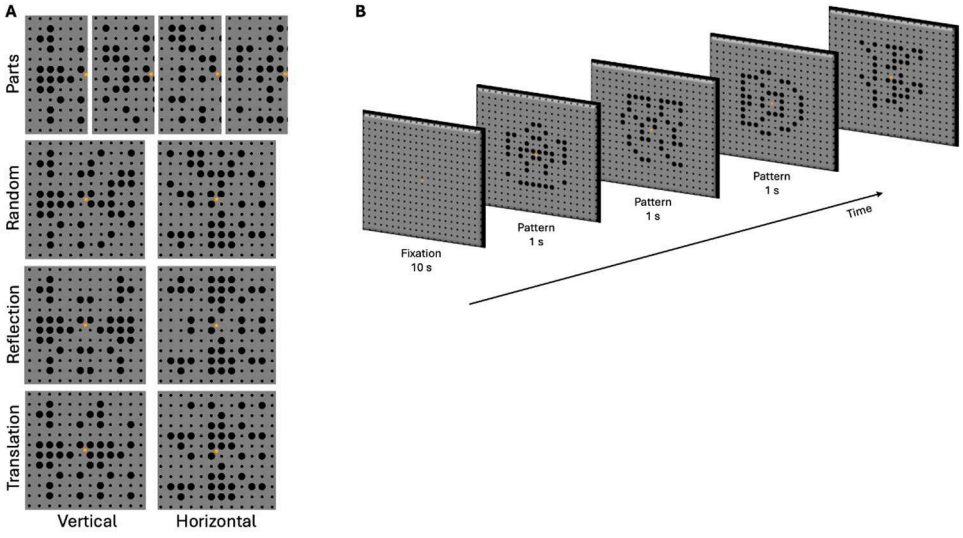

Fig. 1. Examples of dot patterns stimuli used in the experiment. (A) Top: four individual patterns (Parts) are generated for each participant. Parts are then combined with: the mirrored image of a different part to generate random patterns (second row), their corresponding mirrored images to generate reflection patterns (third row), or repeated across to generate translation patterns (bottom). Horizontal axis of symmetry (pattern orientation) was obtained by rotating the original vertical pattern 90 degrees anticlockwise. (B) fMRI design: each experimental run started with 10 s fixation on a regular grid, followed by 1 s stimulus presentations, interleaved by 3–11 s of random patterns. Participants performed, in a counterbalanced order, either a regularity discrimination task or an orientation discrimination task. Based on the feature to be attended, participants indicated via key press whether: the pattern was a reflection vs translation (regularity task); the pattern had vertical vs horizontal orientation axis (orientation task). No key press was expected for random dot patterns.

during regularity discrimination. This would happen if the visual system selectively became view invariant during regularity discrimination, so that horizontal and vertical regularities became the same thing.

1.1. Current study

We first examined the univariate responses to reflection and translation as compared to random dot patterns. We had three univariate predictions.

First, we predicted a robust univariate response to both reflection and translation throughout extrastriate cortex (Prediction 1). This would manifest as a main effect of Region of Interest (ROI) and align with previous fMRI studies (Keefe et al., 2018; Kohler et al., 2016; Sasaki et al., 2005; Tyler et al., 2005; Van Meel et al., 2019; Zamboni et al., 2024) reporting an absent or weak univariate response to regularity (i.e. responses to structured stimuli relative to random patterns) in striate (V1 and V2) cortex.

Second, we predicted that the univariate response to reflection would be stronger than the univariate response to translation in extrastriate ROIs (Prediction 2). This would manifest as a main effect of Regularity Type, and Regularity Type * ROI interaction.

Third, we predicted that the univariate responses in the extrastriate ROIs would be greater in the regularity task than in the orientation task (Prediction 3). This would be supported by a main effect of Task and Task * ROI interaction.

Next, we run more exploratory multivariate analyses. Here predictions were more tentative given the lack of previous research. However, we made three multivariate predictions:

First, we expected regularity type to be decodable from extrastriate regions (Prediction 4).

Second, we predicted orientation would be decodable from V1 (Prediction 5). This would support the claim that feedback from extrastriate areas can 'fill in' the axis in orientation sensitive striate cortex (as suggested by van der Zwan et al., 1998).

Third, we predicted that orientation information would be selectively lost in extrastriate regions during the regularity task (as indirectly suggested by Karakashevska, Bertamini, et al., 2025; Keefe et al., 2018; Makin et al., 2015) (Prediction 6).

We note that we use the term *regularity type* to refer exclusively to the reflection versus translation factor, whereas the more general term *regularity* refers to both types of symmetry (reflection and translation) as a response to structured stimuli, thus averaged across regularity *type,* relative to random pattern stimuli.

2. Materials and methods

2.1. Participants

Twenty-four participants were recruited to the study (mean age 27.2, SD 4.58; 6 male). Data from three participants were removed from the analysis as behavioural performance during scanning was poor, suggesting they either did not understand the instructions or did not pay attention during the experimental trials. The remaining 21 participants had normal or corrected-to-normal visual acuity and no history of neurological impairments. All participants gave written informed consent prior to taking part in the procedure. The study was approved by the York Neuroimaging Centre (YNiC) Research Ethics Committee at the University of York (UK). Each participant underwent two (3 h in total) scanning sessions. The study comprised 72 h of scanning in total.

2.2. Stimuli

Stimuli, presented on a dark grey background, consisted of dot patterns generated using custom-based python scripts. specifically, the full screen was filled with a regular grid of dots (40×23 degrees of visual angle, in size). We were conscious that symmetrical patterns, because of their repeated dot structure, have orientation energy. The ever-present grid therefore reduces the energy contrast related to the axis of the symmetrical patterns. Within the regular grid, a 10×10 square comprising a central subset of the full grid (3.7 degrees of visual angle in size) was selected to contain the patterns. The location of this sub-grid was consistent across trials, while a randomly selected 40 % of dots within the sub-grid were selected as *signal dots* and identified by doubling their size. Similarly to what described in Van Meel et al. (2019), for each participant individually, four 1-fold reflection (i.e., mirror symmetry along the vertical axis) were generated. From these reflection stimuli, each half pattern (heron termed part) was used to generate four vertical translational patterns: the mirror symmetry part was duplicated and translated along the x-axis to obtain a vertical "axis of symmetry". Four unique random patterns were further obtained by combining each part with the mirror reflection of a different part (e.g., part 1 combined with reflection part 2, part 2 combined with reflection part 3, etc.). The resulting 12 stimuli were then rotated 90° anticlockwise to obtain patterns with *horizontal* axis of symmetry (example patterns are provided in Fig. 1).

For each participant, 4 unique patterns per condition (reflection, translation, random) per axis of symmetry (vertical, horizontal) were generated during the first session and each pattern was presented six times throughout one run. Each individual participant was presented with the same patterns throughout the study; however, patterns varied across participants, resulting in a large set of images onto which we base our searchlight Multi-Voxel Pattern Analysis (MVPA), largely reproducing the approach by Van Meel et al. (2019). This design allowed us to decouple orientation information from low-level visual signals by ensuring that the pattern presented did not repeatedly stimulate the same retinotopic locations. Specifically, low-level signals were controlled and randomised in two key ways: 1) by overlaying all patterns on a regular grid background; 2) by generating different signal dot-pairs for each participant. This approach reduced the likelihood that decoding results could be attributed to simple retinotopically driven responses or local luminance differences and increased our confidence that observed effects reflect symmetry-specific processing and not low-level visual features confounds.

The experiment was controlled using Python and open-source Psychopy software (Peirce, 2007). Stimuli were presented using a projector and a mirror setup (1920×1080 pixels resolution, 120 Hz frame rate) at a viewing distance of 62 cm.

2.3. Imaging parameters

All imaging data were acquired on a Siemens MAGNETOM 3T Prisma scanner at the York Neuroimaging Centre (YNiC), University of York, using a 64-channel head coil for both functional and structural data. Each functional run consisted of T2*-weighted echoplanar images (EPIs) (52 slices, resolution 2.5 mm isotropic, TR = 1000 ms, TE = 30 ms, 80×80 acquisition matrix, Multi-Band factor = 4, flip angle = 75 deg).

A T1-weighted high resolution anatomical scan was collected for each participant during the first session (320 slices, resolution 0.8 mm isotropic, TR = 2400 ms, TE = 2.28 ms, FOV = 256 × 256, flip angle = 8 deg). To aid alignment of functional data to the T1-weighted, high resolution anatomical image, a Turbo Spin-Echo image, with the same prescription as the functional data was acquired (52 slices, resolution 1 × 1 × 2.5 mm, TR = 7270 ms, TE = 9.2 ms, FOV = 200 × 200, flip angle = 160 deg).

2.4. Experimental procedure

The study consisted of two separate 1.5-hour sessions. All participants performed both sessions, however three datasets were later removed from analysis due to poor behavioural task performance. Over the course of the two experimental sessions, participants performed a total of 10 runs; 5 runs per session of duration 10 min 20 s. In each

session both tasks were performed alternating from orientation to regularity with the starting task counterbalanced across sessions. Structural scans were obtained during the first session for all participants.

Our stimulus run started and finished with a 10 s period of fixation of an orange dot centred within a rectilinear array of small black dots (Fig. 1B). After the initial period of fixation, stimulus patterns with some of the small dots replaced with larger dots as specified above were presented every 1 s, totally 600 stimuli. Of those stimulus patterns, 96 were targets that were either reflection or translation and had an axis of orientation that was either horizontal or vertical. The 96 targets comprised 16 unique stimuli, four vertical reflection, four horizontal reflection, four vertical translation, four horizontal translation, each repeated six times. The number of random patterns that appeared in between the targets varied from 3 to 11 (that is, an ISI of 3 to 11 s). The stimulus sequence was generated five times for each participant (and repeated across the two sessions). We optimised the stimulus sequence using Optseq2 (https://surfer.nmr.mgh.harvard.edu/optseq).

Participants maintained fixation on an orange central dot throughout the run and performed a discrimination task on (1) the regularity of the patterns where one button was pressed for reflection and another for translation and (2) the orientation of the patterns where one button was pressed for vertical and another for horizontal. Participants were instructed about the tasks to be performed prior to entering the scanner and instructions were displayed on screen before the start of each of the five runs. During each scan, we recorded video of the participant's left eye and later used these recordings to extract eyeblinks using custom-written software (see Vernon et al., 2016). The order of the task to be performed during one experimental session, as well as the keys mapping the reflection / translation and vertical / horizontal responses were counterbalanced within and across participants.

3. Data analyses

3.1. Preprocessing and general linear model

T1-weighted structural data was used for coregistration and 3D cortex reconstruction. Grey and white matter segmentation for each hemisphere was obtained using Freesurfer (https://surfer.nmr.mgh.harvard.edu/) and further manually edited when necessary, using ITKSnap (www.itksnap.org).

All functional data from the main experiment were analysed using FSL FEAT (fMRI Expert Analysis Tool; Jezzard et al., 2001). Preprocessing steps consisted of distortion correction due to non-zero off-resonance field: at the beginning of each functional run, one volume with inverted phase encoding direction was acquired and used to estimate a voxel displacement map, subsequently applied to the functional volumes using FSL topup (Andersson et al., 2003; Smith et al., 2004). Once undistorted, the functional images underwent slice timing correction and high-pass filtering (90 s cut-off point) to remove low-frequency drift. Functional volumes were motion corrected using MCFLIRT and co-registered to each individual's structural image using boundary-based registration tools.

Following preprocessing, a general linear model was applied to the functional images at an individual (first) level, for each task dataset (Orientation, Regularity), separately.

The model consisted of 4 regressors of interest (i.e., one per stimulus condition: reflection vertical & horizontal; translation vertical & horizontal), and six regressors for the motion correction parameters as covariates of no experimental interest. Moreover, a fifth regressor was added to the model accounting for blinks during stimulus presentation, as they have been reported to be potential sources of noise (Gouws et al., 2014; Hupé et al., 2012), as well as response regressor to account for participants pressing response keys to perform the task. Note that, based on the model setup described, the random dot patterns presented during the experimental design are treated as the baseline condition. Thus, contrasts were set up to compare each stimulus category against baseline. To combine data within participant, we ran fixed effects analysis with cluster correction ($Z > 2.3$, $p < 0.05$). Mean percent signal change was then computed by visual area (see Regions of Interest section) using FeatQuery.

3.2. Regions of interest

Multiple regions of interest (ROIs) were identified along the visual cortex based on a probabilistic atlas (Benson et al., 2014). Specifically, each participant's anatomical image was aligned to the anatomical template available from Freesurfer (fsaverage) and the anatomically defined template of visual field maps was applied and further transformed back into each individual anatomical space. This process, implemented via neuropythy, allowed us to obtain the following ROIs: V1, V2, V3, V3a, V3b, V4, VO1, VO2, LO1, LO2, TO1, and TO2. Note that ROIs were defined and analysed bilaterally by combining the left and right hemispheric counterparts into a single region prior to analysis. Because we had no a priori hypotheses regarding hemispheric lateralisation, responses were averaged across hemispheres for each participant, and hemisphere was not included as a factor in the ANOVA. ROIs were further restricted by eccentricity (stimulus size) based on a stimulus vs fixation contrast obtained from the main experiment functional data (across sessions; Fig. 2).

3.3. Searchlight multi voxel pattern analysis

We used multi voxel pattern analysis (MVPA) based on a searchlight technique (Kriegeskorte et al., 2006) to investigate the representation of different regular patterns (i.e., reflection and translation) and their dependence on the orientation of axis of symmetry across the visual cortex. To achieve this, data were processed following the same steps described in Preprocessing and General Linear Model section, but this time implemented in SPM12 (https://www.fil.ion.ucl.ac.uk/spm/software/spm12/). This allowed to easily format data following the structure expected by The Decoding Toolbox (TDT, Hebart et al., 2014), which was then used to perform the searchlight decoding analysis once beta weights for each stimulus condition (reflection vertical, reflection

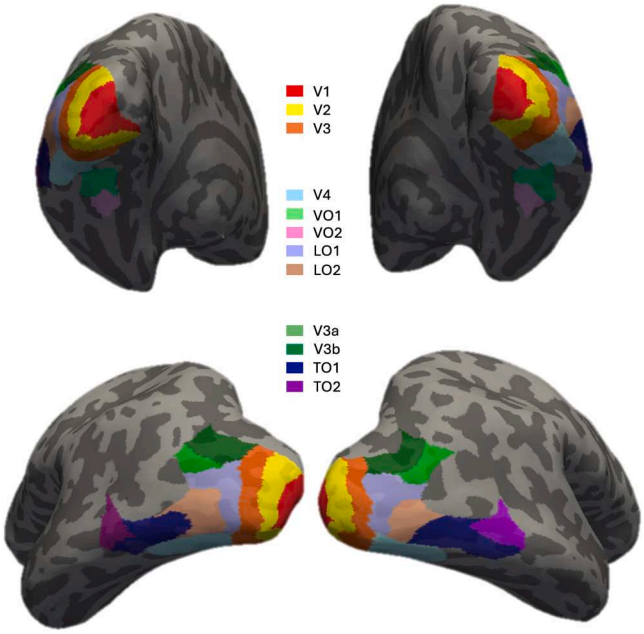

Fig. 2. Regions of Interest. An inflated surface of one representative participant showing the cortical surface of the atlas-defined brain areas used in the ROI-based analysis. Regions from the Benson atlas were mapped onto subjects' space and further restricted by stimulus size.

horizontal, translation vertical, translation horizontal) were estimated. Here we used a linear Support Vector Machines (SVM, Schölkopf et al., 1999) classifier as implemented in TDT to discriminate: (a) reflection from translation patterns; (b) vertical from horizontal axis orientation. The decoding process was performed for data from each participant and each task, i.e., when they were attending to the *regularity* of the patterns vs when they were attending to the *orientation* of the patterns, separately. Classification accuracy for each condition was computed using a leave-one-run-out cross-validation (Kriegeskorte et al., 2009) based on a 5 voxels radius searchlight that iteratively moved across the grey matter voxels of early and higher-level visual cortex identified via a mask spanning occipital, temporal, and parietal cortices.

To perform group-level analysis, the resulting classification accuracy maps were transformed into MNI space (SPM12 normalisation), and these were then used to identify clusters of interest based on the stimulus condition classified (Kriegeskorte et al., 2006). Resulting voxel-wise statistical maps were thresholded at $p < 0.001$ uncorrected (i.e., cluster-extent) and cluster-corrected at $p = 0.05$ family-wise error rate (FWER), unless otherwise stated. Significant clusters were labelled using the automated anatomical labelling (AAL) atlas and Brodmann areas atlas (Glasser et al., 2016).

3.4. Statistical analysis

To test whether the stimulus task combinations had an effect on responses across regions of interest, mean percent signal change values extracted from each ROI (defined bilaterally by combining corresponding left and right hemisphere regions into a single mask) were analysed using a four way repeated measures ANOVA with within-subject factors of ROIs (V1, V2, V3, V3a, V3b, V4, VO1, VO2, LO1, LO2, TO1, TO2), Regularity Type (reflection, translation), Orientation (vertical, horizontal), and Task (regularity discrimination, orientation discrimination). Where violations of sphericity were detected, degrees of freedom were corrected using Greenhouse-Geisser method. Significant main effects and interactions were followed up with planned comparisons or lower-order ANOVAs as appropriate. Effect sizes are reported as partial eta-squared (η^2). Statistical significance was defined at $\alpha = 0.05$ (two-tailed). The p-values resulting from our statistical tests in the univariate analysis were corrected for multiple comparisons using Benjamini-Hochberg False Discovery Rate.

For multivariate searchlight analysis, classification accuracy maps were first computed at the single-participant level as accuracy minus chance (50 %) for each contrast of interest. Group-level inference was performed using one-sample *t*-tests on the accuracy-minus-chance maps to test whether the mean decoding performance across subjects is reliably above chance. Resulting statistical maps were thresholded at $p < 0.001$ (for cluster forming threshold) and corrected for multiple comparisons using family-wise error (FWE) correction at $p < 0.05$. For completeness, uncorrected maps are also reported to visualise sub-thresholds effects.

4. Results

We present the results of our study in the order of our predictions, below, and give a summary table of the predictions and outcomes in Table 1.

4.1. Univariate responses

We first examined the univariate responses to reflectional and translational patterns, contrasted with univariate responses to random patterns. There were four target categories, divided into two regularity types (translation and reflection) and two axes of orientation (horizontal and vertical). There were also two tasks (orientation and regularity). Stimulus-evoked responses to regular patterns contrasted to random patterns, in atlas based, bilaterally defined, visual ROIs are shown in Fig. 3. As predicted, V1 and V2 responses were low across all conditions. There were substantial responses in V3, which were maintained or increased in ROIs further up the visual hierarchy.

Table 1
Overview of study predictions and corresponding results.

Prediction	Analysis	Hypothesis	Key result	Conclusion
1.	Univariate	Extrastriate regions show robust responses to visual regularity	Strong responses from V3 onwards; minimal responses in V1-V2	Supported
2.	Univariate	Reflection > Translation in extrastriate cortex	Translation > Reflection in V3/V3a/V3b	Not supported
3.	Univariate	Regularity task enhances extrastriate responses	No consistent task-related enhancement	Not supported
4.	Multivariate	Regularity type is decodable in extrastriate cortex	Reliable decoding across extrastriate ROIs	Supported
5.	Multivariate	Axis orientation is decodable in early visual cortex	Decoding observed primarily in V1	Partially supported
6.	Multivariate	Orientation information is reduced during regularity discrimination	No consistent reduction observed	Not supported

The responses in Fig. 3A were tested with a four-way repeated measures ANOVA [ROI * Regularity Type * Orientation * Task]. Full ANOVA results are shown in Table 2.

There was a significant main effect of ROI ($p = 9.58\times10–8$) as shown in Fig. 3B There was also a significant main effect of Regularity Type ($p = 0.046$). This resulted from responses to translation being unexpectedly higher than reflection.

There were three significant interactions (Fig. 4). First, there was a significant interaction between ROI and Regularity Type ($p = 1.93\times10–8$). Fig. 4A shows that this was driven by stronger responses to translation in early dorsal areas (V3, V3a, and V3b).

Second, there was an interaction between ROI and Orientation ($p = 0.012$). Fig. 4B shows that this was driven by relatively stronger responses to horizontal patterns in early dorsal areas (V3a and V3b). Conversely, there was significantly greater response to vertical than horizontal patterns in the LO2 region ($p = 0.022$).

Third, there was a significant Task * Orientation interaction ($p = 0.006$). Fig. 4C shows that this interaction was driven by an increased response to vertical than horizontal stimuli in the orientation task. To gain further insight we performed two-way ANOVAs to determine whether the interaction was significant in each ROI. These revealed that the form of the interaction differed across regions. In ventral and lateral visual areas (V2, V4, VO1, VO2, LO1, TO1, and TO2), responses to vertically oriented stimuli were greater than responses to horizontally oriented stimuli during the orientation task. In contrast, dorsal regions (V3 and V3a) showed a different pattern characterised by stronger responses to horizontal than vertical stimuli during the regularity task, together with increased responses to vertically oriented stimuli during the orientation task, relative to the regularity task.

4.2. Multivariate responses

Next, we used multivoxel pattern analysis (MVPA) techniques combined with a searchlight approach to distinguish between: (a) reflection and translation patterns (irrespective of the orientation); and (b) vertical

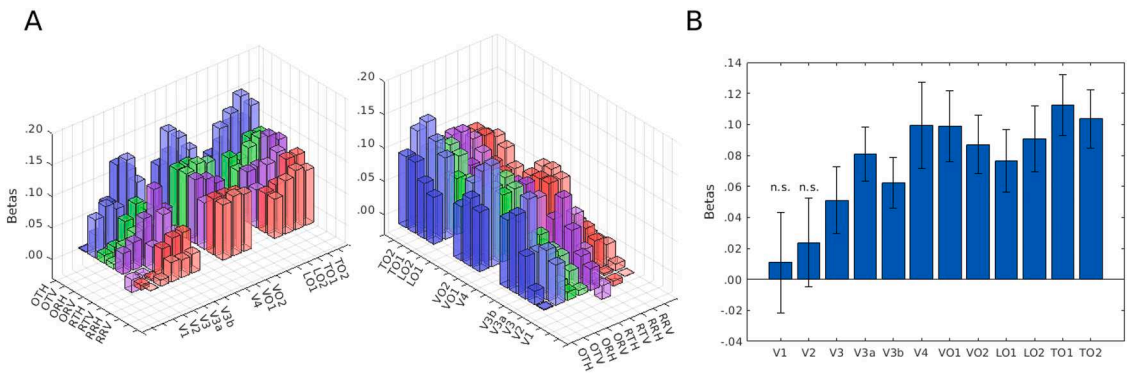

Fig. 3. Overview of univariate results. Responses are shown for bilaterally defined ROIs. (A) Each bar represents a combination of the factors tested. The two panels show the same results set from two viewpoints to ease interpretation of results distributions. The z-axis represents the strength of the response, the y-axis shows the ROIs tested, and the x-axis shows the combination of factors. Blue (translation horizontal and vertical) and Green (reflection horizontal and vertical) bars correspond to the orientation task. Purple (translation horizontal and vertical) and Red (reflection horizontal and vertical) bars correspond to the regularity task. (B) Stimulus-evoked response to regular patterns (reflection & translation, horizontal & vertical) relative to random patterns across tasks for individual areas. Error Bars indicate ±SEM, n.s. indicates statistically non-significant tests.

Table 2
Results of four-way ANOVA. Each row indicates different effects and interactions based on the four factors: ROI, Regularity Type (reflection, translation), Orientation (vertical, horizontal), and Task (regularity, orientation). Bold cells indicate statistical significance ($p < 0.05$); values preceded by asterisks indicate degrees of freedom and p-values following sphericity correction.

ANOVA table **Main effects**	**F**	**df**	**p**	**η^2**
ROI	**12.45**	**11,220** ***3.88,77.6**	**<0.001** ***<0.001**	**.384**
Regularity Type	**4.54**	**1,20**	**.046**	**.185**
Orientation	.051	1,20	.824	.003
Task	.892	1,20	.356	.043

Two-way interactions	**F**	**df**	**p**	**η^2**
ROI * Regularity Type	**5.93**	**11, 220** ***4.62, 92.5**	**<0.001** ***<0.001**	**.229**
ROI * Orientation	**3.70**	**11,220** ***3.48, 69.7**	**<0.000** ***.012**	**.156**
ROI * Task	.066	11, 220 *2.97, 59.4	1.000 *.977	.003
Regularity Type * Task	1.07	1	.313	.051
Orientation * Task	**9.40**	**1**	**.006**	**.320**
Regularity Type * Orientation	0.09	1	.764	.005

Three-way interactions	**F**	**df**	**p**	**η^2**
ROI * Regularity Type * Task	0.35	11, 220 *2.59, 51.8	.971 .756	.017
ROI * Orientation * Task	0.91	11,220 *2.19,43.8	.523 *.414	.044
ROI * Regularity Type * Orientation	0.75	11,220 *1.95,39.0	.689 *.476	.036
Task * Regularity Type * Orientation	2.27	1,20	.148	.102

Four-way Interaction	**F**	**df**	**p**	**η^2**
ROI * Regularity Type * Orientation * Task	2.05	11,220 *2.01,41.3	.025 *.140	.093

and horizontal axes orientation (irrespective of regularity type). We first performed this analysis collapsing over task (Fig. 5) and then for each task separately (Figs. 6 and 7, respectively). While we could reliably decode reflection from translation in extrastriate regions, there was less robust support for our other multivariate predictions.

Decoding accuracy for Regularity Type (irrespective of Orientation and Task), revealed three main clusters: the right superior temporal gyrus, the left inferior temporal gyrus, and left V2 (Fig. 5A& B).

Decoding accuracy for Orientation (irrespective of Regularity Type and Task), revealed no significant clusters with family wise error correction (FWER). However, uncorrected ($p < 0.001$) clusters emerged in left V1, bilateral V2, V3, V4, and V5 (Fig. 5C& D).

Decoding accuracy for Regularity Type was similar in regularity and orientation tasks (Fig. 6A&B vs C&D). However, after FWER correction, some hemispheric differences emerged. This was not predicted and may reflect an 'iceberg' effect, given the largely symmetrical brain regions that are capable of decoding in the uncorrected brain maps.

Decoding accuracy for Orientation was also similar across tasks. We observed clusters in early visual cortex, including V1, bilateral V2, and V3 during both regularity and orientation tasks (Fig. 7A&B vs C&D). It is important to note that these clusters emerged following a cluster-extent correction of $p < 0.001$ and did not survive FWER correction.

5. Discussion

In this study, participants viewed dot patterns belonging to two types of regularity; reflection and translation, amidst random dot configurations, on a background regular grid of dots. These regular patterns were generated to have horizontal and vertical axes of orientation. Stimuli were presented under a regularity (reflection vs translation) discrimination task, or an orientation (vertical vs horizontal axis of orientation) discrimination task. Using this design, we examined how stimulus regularity type, axis of orientation of the regularity, and task demands modulate responses across the striate and extrastriate visual cortex, using both univariate and multivariate analyses.

First, we predicted robust univariate responses to both reflection and translation in extrastriate cortex, with little or no response in striate cortex (Prediction 1). This prediction was supported: stimulus-evoked responses to regular patterns relative to random patterns are minimal in V1 and V2, rather they emerge in V3 and beyond.

Second, we predicted stronger univariate responses to reflection than translation in extrastriate regions (Prediction 2). This prediction was not supported. Instead, early dorsal ROIs (V3, V3a, V3b) showed greater responses to translation than reflection patterns.

Third, we predicted that univariate responses in extrastriate cortex would be enhanced during the regularity task relative to the orientation task (Prediction 3). While this was not supported, we show that responses to orientation varied with ROI. Early dorsal regions (V3a and V3b) show greater responses to horizontal stimuli and area LO2 shows greater responses to vertical stimuli. Finally, response to vertically oriented stimuli were enhanced during the orientation task compared to the regularity task, except in areas V1, V3b, and LO2 where this trend did not reach statistical significance. We discuss each result below.

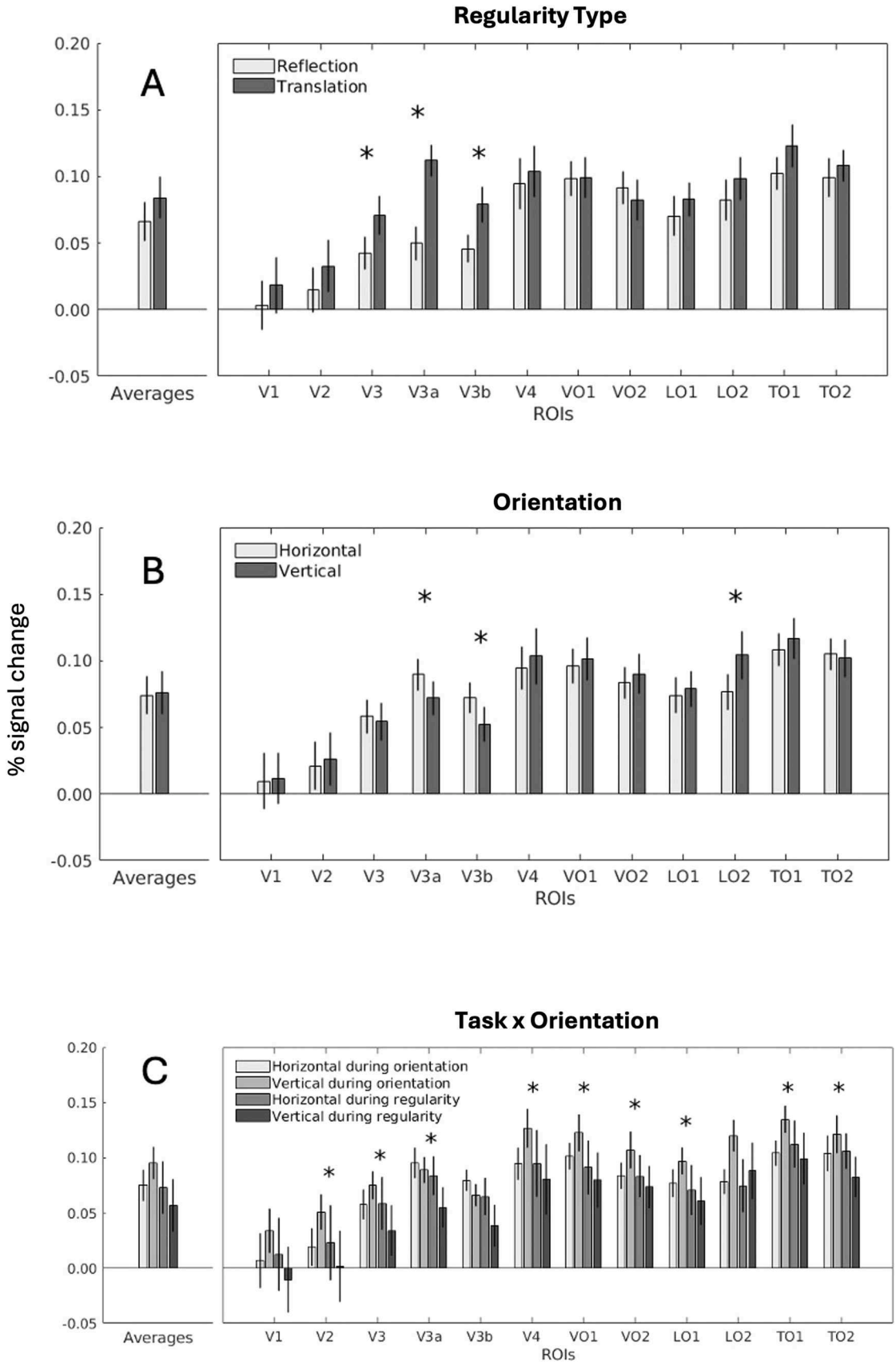

Fig. 4. Univariate results for (A) interaction between ROI and regularity type (reflection in light grey, translation in dark grey). Early dorsal visual areas show stronger responses to translation. (B) Interaction between ROI and orientation (horizontal in light grey, vertical in dark grey). Dorsal areas show stronger responses to horizontal, while area LO2 shows the reverse pattern. (C) Interaction between task (regularity in darker shades, orientation in lighter shades) and orientation (horizontal in lighter shades, vertical in darker shades). Error bars indicate ±SEM. Asterisks indicate statistical significance.

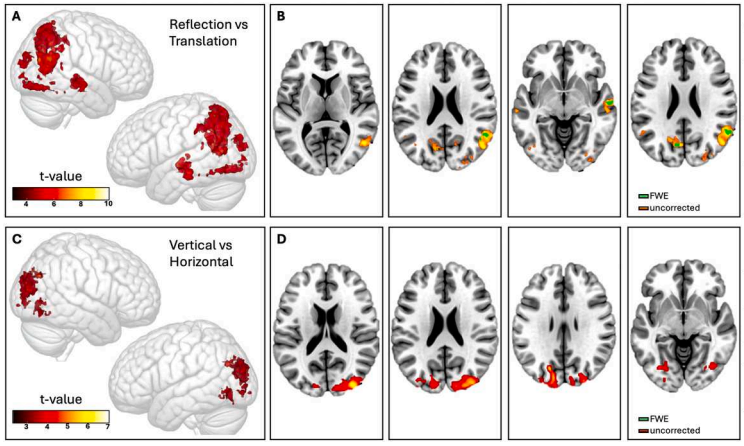

Contrast	Region	Hemi	Peak (x, y, z)	t	p_FWER	Accuracy – chance (μ, SEM)
Reflection > Translation	**V2**	L	–4, –70, 24	8.47	.010	4.18 ± 0.49
	Fusiform	R	50, –62, 8	10.30	<.001	5.52 ± 0.53
	Superior temporal gyrus	R	58, –12, –6	8.85	.005	5.17 ± 0.58
	Inferior temporal gyrus	L	–56, –26, –16	7.29	.029	4.99 ± 0.63
	Angular gyrus	R	50, –68, 22	9.47	.002	5.24 ± 0.53
Vertical > Horizontal	V1	L	–6, –98, –6	4.64	1.000	3.63 ± 0.78
	V2	L	–18, –70, 28	6.51	.511	3.55 ± 0.54
	V3/4/5	R	34, –84, 18	7.26	.108	3.84 ± 0.53
		L	–26, –84, 22	5.57	1.000	3.1 ± 0.55

Fig. 5. Task-independent searchlight results. A and B: Brain maps show clusters with higher than chance accuracy when decoding reflection vs translation across tasks. Uncorrected (hot colour map, $p < 0.001$) t-statistical map showing clusters spanning ventral and dorsal visual cortex. Contours in green overlaid on top of uncorrected maps highlight the significant clusters shown in the table to the right of the figure following FWER correction for multiple comparisons ($p < 0.05$). C and D: Brain maps showing clusters (cluster-extent corrected at $p < 0.001$) with higher than chance accuracy when decoding axis orientation (vertical vs horizontal) across tasks. Clusters here span early visual cortex, expanding along the dorsal pathway (see Table on the right of the figure for MNI coordinates and individual values).

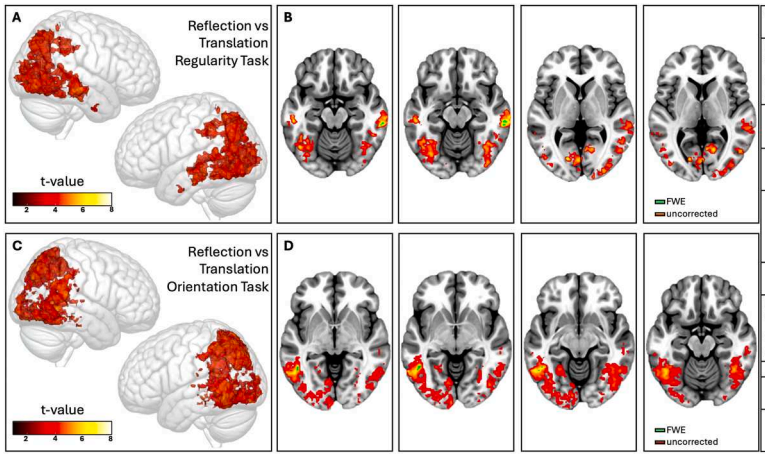

Contrast	Region	Hemi	Peak (x, y, z)	t	p_FWER	Accuracy – chance (μ, SEM)
Reflection > Translation (Regularity task)	**V2**	L	–16, –76, 2	7.96	0.027	3.99 ± 0.50
	V3/4/5	R	26, –72, 38	6.86	0.246	5.28 ± 0.77
		L	-40, -82, 4	5.15	1.000	4.99 ± 0.97
	Middle temporal gyrus	L	–52, –28, –4	4.78	1.000	3.92 ± 0.82
	Inferior temporal gyrus	L	–52, –22, –22	7.52	0.064	5.54 ± 0.73
		R	64, -30, -16	9.14	0.003	4.43 ± 0.48
	Supramarginal gyrus	R	58, –44, 34	5.15	1.000	5.33 ± 1.03
Reflection > Translation (Orientation task)	V2	R	30, –94, –6	4.61	1.000	4.40 ± 0.95
	V3/4/5	R	30, –84, –6	4.39	1.000	5.37 ± 1.22
	Fusiform gyrus	L	–46, –50, –4	9.02	0.004	6.08 ± 0.75
	Inferior temporal gyrus	L	–58, –34, –12	4.85	1.000	4.09 ± 0.84

Fig. 6. Regularity Type by Task searchlight results. A and B: Brain maps show clusters with higher than chance accuracy when decoding reflection vs translation during Regularity task. Uncorrected (hot colour map, $p < 0.001$) t-statistical map showing clusters along the ventral visual pathway. Contours in green overlaid on top of the uncorrected map highlight the significant clusters shown in the table to the right of the figure following FWER correction for multiple comparisons ($p < 0.05$). C and D: Brain maps show clusters (cluster-extent corrected at $p < 0.001$, hot colour map, in green clusters following FWER correction at $p < 0.05$) with higher than chance accuracy when decoding reflection vs translation during the Orientation task. Areas in the ventral visual pathway (see Table to the right for MNI coordinates and cluster values) show encoding of regularity type.

Stimulus-evoked responses to regular patterns, compared to random patterns, emerged primarily in extrastriate visual areas while remaining largely absent or very limited in early visual cortex (V1 and V2). This was entirely expected and aligns with previous fMRI studies showing that regularity responses (i.e., responses to stimuli defined by a regular feature, e.g. reflection, translation, rotation) are most present in regions such as V4, VO1, and LOC (Audurier et al., 2022; Keefe et al., 2018; Kohler et al., 2016; Sasaki et al., 2005; Tyler et al., 2005; Van Meel et al., 2019; Zamboni et al., 2024). There is therefore a relatively strong consensus that V1 does not compute regularity, but V3 does and V2 could possibly be involved.

Contrary to prediction 2, early dorsal regions (V3, V3a, and V3b) showed stronger responses to translation than reflection. This could be because translation patterns were interpreted as two objects, and reflection patterns were interpreted as one object. The dorsal stream provides input to the posterior parietal cortex that is sensitive to numerosity and consequent affordances (Harvey et al., 2013). It is possible that some preservation of the coding of the number of items in the dorsal stream, so that reflection and translation may be perceived as one and two objects, respectively, is at the base of this result.

We did not observe a larger univariate response for reflection than translation at any extrastriate ROI, despite the well-reported effect that reflection is more salient than translation. This was noted over a century ago by Ernst Mach (1886) and more recent theoretical accounts suggest reflection has higher 'perceptual goodness' than translation (van der Helm and Leeuwenberg, 1996). Furthermore, reflection is more easily discriminated in psychophysical studies (Baylis and Driver, 2001; Bertamini et al., 1997; Koning and Wagemans, 2009) and reflection generates a larger SPN in ERP studies (Makin et al., 2013, 2014, 2016). Finally, some fMRI evidence also supports that reflection is more perceptually salient than stimuli with translated elements (supporting Fig. 7 of Sasaki et al., 2005). While explaining the absence of a result is always a challenge, a potential explanation might come from the way in which we presented our stimuli. Indeed, these were embedded within a dense, regular grid that was present throughout the experiment. While this manipulation was intended to control low-level orientation energy,

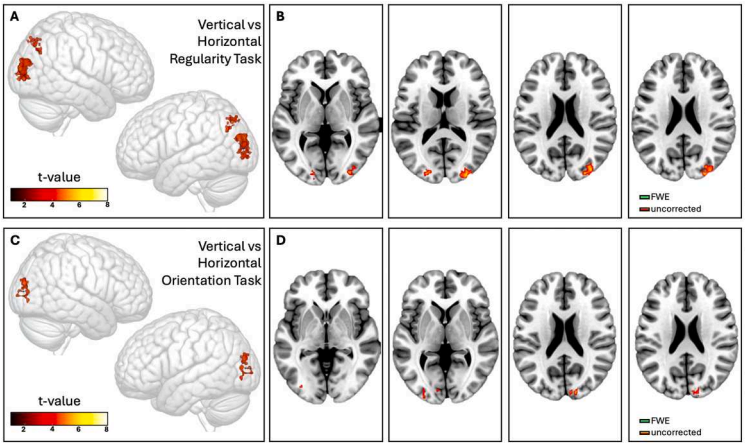

Contrast	Region	Hemi	Peak (x, y, z)	t	p_FWER	Accuracy – chance (μ, SEM)
Vertical > Horizontal (Regularity task)	V1	L	–14, –90, 2	4.69	1.000	5.23 ± 1.11
	V2	R	30, –92, 14	5.91	1.000	4.61 ± 0.78
	V3/4/5	R	34, –84, 20	5.88	1.000	4.54 ± 0.77
		L	-18, -86, 14	4.94	1.000	4.48 ± 0.90
Vertical > Horizontal (Orientation task)	V1	L	–8, –86, 2	4.46	1.000	3.98 ± 0.89
	V2	R	16, –88, 20	6.02	1.000	4.73 ± 0.78
		L	-28, -94, 2	4.21	1.000	3.94 ± 0.93
	V3/4/5	L	–32, –82, –2	4.68	1.000	3.88 ± 0.83

Fig. 7. Axis symmetry by Task searchlight results. A and B: Brain maps show clusters with higher than chance accuracy when decoding vertical vs horizontal axis of symmetry during the Regularity task. Uncorrected ($p < 0.001$) t-statistical map showing clusters in the primary visual cortex, as well as dorsal pathway. C and D: Brain maps show clusters with higher than chance accuracy when decoding axis symmetry during the Orientation task. Uncorrected ($p < 0.001$) t-statistical map showing a similar cluster extent to A&B. The Table to the right reports the corresponding cluster MNI coordinates and values. Note that these clusters did not survive FWER correction.

it may also have reduced the perceptual differences in salience between reflection and translation by making both appear as perturbations of highly structured background. Another possibility is that our grid context provided a repeating lattice texture, thus when both reflection and translation stimuli are embedded in this periodic grid, the translation component becomes salient for both conditions, potentially equalising responses that would otherwise favour reflection in isolated or irregular contexts.

Analysis of task manipulation shows that task has no effect here (Prediction 3). While the SPN is usually largest during regularity discrimination, this is reduced, but not abolished, during various secondary tasks (Makin et al., 2024; Makin et al., 2020, 2022). In our case, however, the absence of a task effect could be due to the essence of the tasks used: To determine whether the orientation was horizontal or vertical in the orientation task, one must first find the global axis. This means that regularity was not irrelevant in the orientation task, thus creating an interdependence that could have overshadowed the effect of task.

The interaction between ROI and Orientation is also noteworthy. Dorsal regions showed stronger responses to horizontal, and LO2 showed stronger responses to vertical axis orientation. The preference in LO2 for vertical axis stimuli is consistent with its strong stimulus-evoked response to regular stimuli (Fig. 3B) relative to random patterns. Indeed regularity (i.e., a stimulus presenting reflection or translation features) is processed more efficiently, compared to a random stimulus configuration, when presented vertically and is experienced most frequently in natural images and biological subjects (Palmer and Hemenway, 1978; Wenderoth, 1994). The dorsal stream preference for horizontal, on the other hand, is harder to explain. Areas V3A and V3B are strongly implicated in spatial integration, motion, and 3D structure, and are thought to support the organisation of visual information across large portions of the visual field, especially in relation to "perception for action" (Ayzenberg and Behrmann, 2022; Sakata et al., 1998). In these regions, axis orientation may matter primarily because it changes the spatial integration problem, e.g., whether information can be integrated largely within one hemisphere (horizontal axes) or must be coordinated across hemispheres (vertical axes). Thus, the preference for horizontal axes in V3A / V3B may reflect reduced demands on large-scale spatial integration.

Our multivariate results complemented the univariate observations above. As expected, we found above chance decoding of regularity type in extrastriate regions (Prediction 4). This was a robust finding, which survived correction for familywise error rate. Other aspects of the multivariate results were less conclusive.

We found above chance decoding of orientation in early visual cortex, as expected (Prediction 5). This is consistent with feedback from extrastriate cortex (which processes stimulus-related regularity properties) to early visual cortex (which processes orientation), as suggested by van der Zwan et al. (1998). Although this result only reached significance without correction for familywise error rate, it is broadly consistent with predictions. It is not clear why left V1 should code orientation better than right V1. This hemispheric asymmetry was not expected. One possibility is that this reflects statistical variability in a weak bilateral effect, such that only the left hemisphere crossed the cluster-level threshold – an 'iceberg' effect in which subthreshold effects are present bilaterally but only one side survives correction. This, paired with the fact that we did not explicitly test the superiority of left, over right hemisphere in orientation coding, should not be interpreted as evidence for apparent lateralisation, but rather consider replications with designs optimised to isolate feedback-related orientation coding.

We had tentatively expected to decode orientation from extrastriate regions during the orientation task, but not during regularity task (Prediction 6). This result would be conceptually consistent with previous research on task selective view invariance (Karakashevska, Batterley, et al., 2025, 2025; Karakashevska and Makin, 2024; Keefe et al., 2018; Makin et al., 2015; Rampone et al., 2019). However, we could not reliably decode orientation from any extrastriate region in either task. Nevertheless, without correcting for familywise error rate, V4 shows some orientation sensitivity in both tasks. This could be interpreted as lack of view invariance, albeit without the expected task selectivity.

The more robust decoding regularity type highlights the ability of the extrastriate regions to extract regularity features in patterns that are well matched for low level features. The less robust decoding of orientation in earlier regions may be due to the fact these regions were responding to all stimuli. Potentially present stimuli at lower contrast to reduce ceiling effects in early regions could have helped untangle this outcome.

Notwithstanding this limitation, our stimuli had merits. The larger elements were overlaid on a regular grid background. This minimised low-level visual feature confounds and ensured that decoding reflected regularity-specific processing rather than retinotopic or luminance differences. Moreover, the use of a regular grid present throughout the experiment controlled for local orientation energy and isolated orientation effects related to the axis of symmetry.

6. Conclusion

In summary, this study replicated the standard univariate extrastriate symmetry response for both reflectional and translational symmetry. Unexpectedly, these univariate responses were similar in most extrastriate regions, and translation produced a larger response in early dorsal areas V3, V3a, and V3b. Multivariate analysis revealed differential coding of reflection and translation in several extrastriate regions. Finally, we observed modest evidence that axis orientation information is fed back to V1, in keeping with previous studies on tilt aftereffects.

Open research - data availability statement

The summary data, stimulus presentation & analysis code of this study will be made available on Open Science Framework upon publication. fMRI data will be made available on OpenNeuro upon publication.

Funding statement

The project was funded by an ESRC grant (ES/S014691/1) to ADJ Makin (PI), AB Morland (CoI), and M Bertamini (CoI).

Data and code availability statement

The summary data, stimulus presentation & analysis code of this study will be made available on Open Science Framework upon publication. fMRI data will be made available on OpenNeuro upon publication.

CRediT authorship contribution statement

E. Zamboni: Writing – review & editing, Writing – original draft, Visualization, Validation, Methodology, Investigation, Formal analysis, Data curation, Conceptualization. **R. Lowndes:** Writing – review & editing, Writing – original draft, Visualization, Validation, Formal analysis, Data curation. **M. Bertamini:** Writing – review & editing, Writing – original draft, Supervision, Project administration, Investigation, Funding acquisition, Conceptualization. **A.D.J. Makin:** Writing – review & editing, Writing – original draft, Project administration, Investigation, Funding acquisition, Conceptualization. **A.B. Morland:** Writing – review & editing, Writing – original draft, Supervision, Project administration, Investigation, Funding acquisition, Conceptualization.

Declaration of competing interest

We have no conflict to declare.

Acknowledgements

We thank the staff at the York Neuroimaging Centre, Dr Isaac Watson, and Dr Aneurin Kennerley for support with MRI scanning. We have no conflict to declare.

References

Andersson, J.L.R., Skare, S., Ashburner, J., 2003. How to correct susceptibility distortions in spin-echo echo-planar images: application to diffusion tensor imaging. Neuroimage 20 (2), 870–888. https://doi.org/10.1016/S1053-8119(03)00336-7.

Audurier, P., Héjja-Brichard, Y., De Castro, V., Kohler, P.J., Norcia, A.M., Durand, J.-B., Cottereau, B.R., 2022. Symmetry processing in the macaque visual cortex. In: Cereb. Cortex (New York, N.Y.: 1991), 32, pp. 2277–2290. https://doi.org/10.1093/cercor/bhab358.

Ayzenberg, V., Behrmann, M., 2022. The dorsal visual pathway represents object-centered spatial relations for object recognition. J. Neurosci. 42 (23), 4693–4710. https://doi.org/10.1523/JNEUROSCI.2257-21.2022.

Baylis, G.C., Driver IV, J., 2001. Perception of symmetry and repetition within and across visual shapes: part-descriptions and object-based attention. Vis. Cogn. 8 (2), 163–196. https://doi.org/10.1080/13506280042000126.

Benson, N.C., Butt, O.H., Brainard, D.H., Aguirre, G.K., 2014. Correction of distortion in flattened representations of the cortical surface allows prediction of V1-V3 functional organization from anatomy. PLoS Comput. Biol. 10 (3), e1003538. https://doi.org/10.1371/journal.pcbi.1003538.

Bertamini, M., Friedenberg, J.D., Kubovy, M., 1997. Detection of symmetry and perceptual organization: the way a lock-and-key process works. Acta Psychol. 95 (2), 119–140. https://doi.org/10.1016/s0001-6918(96)00038-8.

Bertamini, M., Silvanto, J., Norcia, A.M., Makin, A.D.J., Wagemans, J., 2018. The neural basis of visual symmetry and its role in mid- and high-level visual processing. Ann. N. Y. Acad. Sci. 1426 (1), 111–126. https://doi.org/10.1111/nyas.13667.

Contemori, G., Musa, M., Demirkapi, D., Passaggi, M., Oletto, C.M., Battaglini, L., Bertamini, M., 2026. Sustained posterior negativity (SPN) elicited by brief (20 ms) symmetrical stimuli. Front. Psychol. 16 (1657531). https://doi.org/10.3389/fpsyg.2025.1657531.

Glasser, M.F., Coalson, T.S., Robinson, E.C., Hacker, C.D., Harwell, J., Yacoub, E., Ugurbil, K., Andersson, J., Beckmann, C.F., Jenkinson, M., Smith, S.M., Van Essen, D. C., 2016. A multi-modal parcellation of human cerebral cortex. Nature 536 (7615), 171–178. https://doi.org/10.1038/nature18933.

Gouws, A.D., Alvarez, I., Watson, D.M., Uesaki, M., Rodgers, J., Morland, A.B., 2014. On the role of suppression in spatial attention: evidence from negative BOLD in human subcortical and cortical structures. J. Neurosci. 34 (31), 10347–10360. https://doi.org/10.1523/JNEUROSCI.0164-14.2014.

Harvey, B.M., Klein, B.P., Petridou, N., Dumoulin, S.O., 2013. Topographic representation of numerosity in the human parietal cortex. Science 341 (6150), 1123–1126. https://doi.org/10.1126/science.1239052.

Hebart, M.N., Görgen, K., Haynes, J.-D., 2014. The decoding Toolbox (TDT): a versatile software package for multivariate analyses of functional imaging data. Front. Neuroinform. 8, 88. https://doi.org/10.3389/fninf.2014.00088.

Hupé, J.-M., Bordier, C., Dojat, M., 2012. A BOLD signature of eyeblinks in the visual cortex. Neuroimage 61 (1), 149–161. https://doi.org/10.1016/j.neuroimage.2012.03.001.

Jacobsen, T., Höfel, L., 2003. Descriptive and evaluative judgment processes: behavioral and electrophysiological indices of processing symmetry and aesthetics. Cogn. Affect. Behav. Neurosci. 3 (4), 289–299. https://doi.org/10.3758/cabn.3.4.289.

Jezzard, P., Matthews, P.M., & Smith, S.M. (2001). *Functional MRI: an introduction to methods*.

Karakashevska, E., Batterley, M., Yao, Y., Makin, A.D.J., 2025a. They look virtually the same: extraretinal representation of symmetry in virtual reality. Cortex 189, 59–75. https://doi.org/10.1016/j.cortex.2025.05.008.

Karakashevska, E., Bertamini, M., Makin, A.D.J., 2025b. Putting things into perspective: which visual cues facilitate automatic extraretinal symmetry representation? Cortex 184, 131–149. https://doi.org/10.1016/j.cortex.2024.11.024.

Karakashevska, E., Makin, A.D.J., 2024. Polygons have a small facilitatory effect on extraretinal symmetry perception. Neuroimage 302 (120894), 120894. https://doi.org/10.1016/j.neuroimage.2024.120894.

Keefe, B.D., Gouws, A.D., Sheldon, A.A., Vernon, R.J.W., Lawrence, S.J.D., McKeefry, D. J., Wade, A.R., Morland, A.B., 2018. Emergence of symmetry selectivity in the visual areas of the human brain: fMRI responses to symmetry presented in both frontoparallel and slanted planes. Hum. Brain Mapp. 39 (10), 3813–3826. https://doi.org/10.1002/hbm.24211.

Kohler, P.J., Clarke, A., Yakovleva, A., Liu, Y., Norcia, A.M., 2016. Representation of maximally regular textures in Human visual cortex. J. Neurosci. 36 (3), 714–729. https://doi.org/10.1523/JNEUROSCI.2962-15.2016.

Koning, A., Wagemans, J., 2009. Detection of symmetry and repetition in one and two objects. Structures versus strategies. Exp. Psychol. 56 (1), 5–17. https://doi.org/10.1027/1618-3169.56.1.5.

Kriegeskorte, N., Goebel, R., Bandettini, P., 2006. Information-based functional brain mapping. Proc. Natl. Acad. Sci. U.S.A. 103 (10), 3863–3868. https://doi.org/10.1073/pnas.0600244103.

Kriegeskorte, N., Simmons, W.K., Bellgowan, P.S.F., Baker, C.I., 2009. Circular analysis in systems neuroscience: the dangers of double dipping. Nat. Neurosci. 12 (5), 535–540. https://doi.org/10.1038/nn.2303.

Mach, E., 1886. The Analysis of Sensations and the Relation of the Phsysical to the Psychical. Dover.

Makin, A.D.J., Buckley, N., Austin, E., Bertamini, M., 2024. When does perceptual organization happen? Cortex 174, 70–92. https://doi.org/10.1016/j.cortex.2024.02.007.

Makin, A.D.J., Rampone, G., Bertamini, M., 2015. Conditions for view invariance in the neural response to visual symmetry. Psychophysiology. 52 (4), 532–543. https://doi.org/10.1111/psyp.12365.

Makin, A.D.J., Rampone, G., Morris, A., Bertamini, M., 2020. The formation of symmetrical gestalts is task-independent, but can be enhanced by active regularity discrimination. J. Cogn. Neurosci. 32 (2), 353–366. https://doi.org/10.1162/jocn_a_01485.

Makin, A.D.J., Rampone, G., Pecchinenda, A., Bertamini, M., 2013. Electrophysiological responses to visuospatial regularity. Psychophysiology. 50 (10), 1045–1055. https://doi.org/10.1111/psyp.12082.

Makin, A.D.J., Rampone, G., Wright, A., Martinovic, J., Bertamini, M., 2014. Visual symmetry in objects and gaps. J. Vis. 14 (3), 12. https://doi.org/10.1167/14.3.12.

Makin, A.D.J., Roccato, M., Karakashevska, E., Tyson-Carr, J., Bertamini, M., 2023. Symmetry perception and psychedelic experience. Symmetry (Basel) 15 (7), 1340. https://doi.org/10.3390/sym15071340.

Makin, A.D.J., Tyson-Carr, J., Rampone, G., Derpsch, Y., Wright, D., Bertamini, M., 2022. Lessons from a catalogue of 6674 brain recordings. Elife 11. https://doi.org/10.7554/eLife.66388.

Makin, A.D.J., Wright, D., Rampone, G., Palumbo, L., Guest, M., Sheehan, R., Cleaver, H., Bertamini, M., 2016. An electrophysiological index of perceptual goodness. In: Cereb. Cortex (New York, N.Y.: 1991), 26, pp. 4416–4434. https://doi.org/10.1093/cercor/bhw255.

Palmer, S.E., Hemenway, K., 1978. Orientation and symmetry: effects of multiple, rotational, and near symmetries. J. Exp. Psychol. Hum. Percept. Perform. 4 (4), 691–702. https://doi.org/10.1037//0096-1523.4.4.691.

Palumbo, L., Bertamini, M., Makin, A., 2015. Scaling of the extrastriate neural response to symmetry. Vision Res. 117, 1–8. https://doi.org/10.1016/j.visres.2015.10.002.

Peirce, J.W., 2007. PsychoPy–psychophysics software in Python. J. Neurosci. Methods 162 (1–2), 8–13. https://doi.org/10.1016/j.jneumeth.2006.11.017.

Rampone, G., Makin, A.D.J., Tatlidil, S., Bertamini, M., 2019. Representation of symmetry in the extrastriate visual cortex from temporal integration of parts: an EEG/ERP study. Neuroimage 193, 214–230. https://doi.org/10.1016/j.neuroimage.2019.03.007.

Sakata, H., Taira, M., Kusunoki, M., Murata, A., Tanaka, Y., Tsutsui, K., 1998. Neural coding of 3D features of objects for hand action in the parietal cortex of the monkey. Philos. Trans. R. Soc. Lond., B, Biol. Sci. 353 (1373), 1363–1373. https://doi.org/10.1098/rstb.1998.0290.

Sasaki, Y., Vanduffel, W., Knutsen, T., Tyler, C., Tootell, R., 2005. Symmetry activates extrastriate visual cortex in human and nonhuman primates. Proc. Natl. Acad. Sci. U. S.A. 102 (8), 3159–3163. https://doi.org/10.1073/pnas.0500319102.

Sawada, T., Pizlo, Z., 2008. Detection of skewed symmetry. J. Vis. 8 (5), 14.1–1418. https://doi.org/10.1167/8.5.14.

Schölkopf, B., Mika, S., Burges, C.C., Knirsch, P., Müller, K.R., Rätsch, G., Smola, A.J., 1999. Input space versus feature space in kernel-based methods. IEEe Trans. Neural Netw. 10 (5), 1000–1017. https://doi.org/10.1109/72.788641.

Smith, S.M., Jenkinson, M., Woolrich, M.W., Beckmann, C.F., Behrens, T.E.J., Johansen-Berg, H., Bannister, P.R., De Luca, M., Drobnjak, I., Flitney, D.E., Niazy, R.K., Saunders, J., Vickers, J., Zhang, Y., De Stefano, N., Brady, J.M., Matthews, P.M., 2004. Advances in functional and structural MR image analysis and implementation as FSL. Neuroimage 23 (Suppl 1), S208–S219. https://doi.org/10.1016/j.neuroimage.2004.07.051.

Szlyk, J.P., Rock, I., Fisher, C.B., 1995. Level of processing in the perception of symmetrical forms viewed from different angles. Spat. Vis. 9 (1), 139–150. https://doi.org/10.1163/156856895×00151.

Treder, M.S., 2010. Behind the looking-glass: a review on human symmetry perception. Symmetry (Basel) 2 (3), 1510–1543. https://doi.org/10.3390/sym2031510.

Tyler, C.W., Baseler, H.A., Kontsevich, L.L., Likova, L.T., Wade, A.R., Wandell, B.A., 2005. Predominantly extra-retinotopic cortical response to pattern symmetry. Neuroimage 24 (2), 306–314. https://doi.org/10.1016/j.neuroimage.2004.09.018.

van der Helm, P.A., Leeuwenberg, E.L.J., 1996. Goodness of visual regularities: a nontransformational approach. Psychol. Rev. 103 (3), 429–456. https://doi.org/10.1037/0033-295x.103.3.429.

van der Vloed, G., Csathó, A., van der Helm, P.A., 2005. Symmetry and repetition in perspective. Acta Psychol. 120 (1), 74–92. https://doi.org/10.1016/j.actpsy.2005.03.006.

van der Zwan, R., Leo, E., Joung, W., Latimer, C., Wenderoth, P., 1998. Evidence that both area V1 and extrastriate visual cortex contribute to symmetry perception. Curr. Biol. 8 (15), 889–892. https://doi.org/10.1016/s0960-9822(07)00353-3.

Van Meel, C., Baeck, A., Gillebert, C.R., Wagemans, J., Op de Beeck, H.P., 2019. The representation of symmetry in multi-voxel response patterns and functional connectivity throughout the ventral visual stream. Neuroimage 191, 216–224. https://doi.org/10.1016/j.neuroimage.2019.02.030.

Vernon, R.J.W., Gouws, A.D., Lawrence, S.J.D., Wade, A.R., Morland, A.B., 2016. Multivariate patterns in the human object-processing pathway reveal a shift from retinotopic to shape curvature representations in lateral occipital areas, LO-1 and LO-2. J. Neurosci. 36 (21), 5763–5774. https://doi.org/10.1523/JNEUROSCI.3603-15.2016.

Wenderoth, P., 1994. The salience of vertical symmetry. Perception. 23 (2), 221–236. https://doi.org/10.1068/p230221.

Zamboni, E., Makin, A.D.J., Bertamini, M., Morland, A.B., 2024. The role of task on the human brain's responses to, and representation of, visual regularity defined by reflection and rotation. Neuroimage 297 (120760), 120760. https://doi.org/10.1016/j.neuroimage.2024.120760.